

# Face Identification with Bilinear CNNs

Aruni RoyChowdhury<sup>1</sup>, Tsung-Yu Lin<sup>1</sup>, Subhransu Maji<sup>1</sup>, and Erik Learned-Miller<sup>1</sup>

<sup>1</sup>College of Information and Computer Sciences

University of Massachusetts, Amherst

## Abstract

The recent explosive growth in convolutional neural network (CNN) research has produced a variety of new architectures for deep learning. One intriguing new architecture is the bilinear CNN (BCNN), which has shown dramatic performance gains on certain fine-grained recognition problems [13]. We apply this new CNN to the challenging new face recognition benchmark, the IARPA Janus Benchmark A (IJB-A) [10]. This is the first widely available public benchmark designed specifically to test face identification in real-world images. It features faces from a large number of identities in challenging real-world conditions. Because the face images were not identified automatically using a computer face detection system, it does not have the bias inherent in such a database. As a result, it includes variations in pose that are more challenging than many other popular benchmarks. In our experiments, we demonstrate the performance of the model trained only on ImageNet, then fine-tuned on the training set of IJB-A, and finally use a moderate-sized external database, FaceScrub [15]. Another feature of this benchmark is that the testing data consists of *collections* of samples of a particular identity. We consider two techniques for pooling samples from these collections to improve performance over using only a single image, and we report results for both methods. Our application of this new CNN to the IJB-A results in gains over the published baselines of this new database.

## 1 Introduction

Since the introduction of the Labeled Faces in the Wild (LFW) database [7], there has been intense interest in the problem of unconstrained face *verification*. In this problem, the goal is to determine whether two face images represent the same individual or not. From initial recognition rates in the low seventies [16], recent algorithms are achieving rates of over 99% using a variety of different methods [20, 21, 24].

While face verification has been an interesting research problem, a protocol more closely aligned with real-world applications is face *identification*. In this scenario, visual information is gathered about a set of known subjects (the *gallery*), and at test time, a new subject (the *probe*) is presented. The goal is to determine which member of the gallery, if any, is represented by the probe. When the tester guarantees that the probe is among the gallery identities, this is known as *closed set identification*. When the probes may include those who are not in the gallery, the problem is referred to as *open set identification*.

Since verification accuracy rates on LFW are rapidly approaching 100%, there has been strong demand for a new identification protocol that can push face recognition forward again. The new

IARPA Janus Benchmark A (IJB-A) is designed to satisfy this need. The IJB-A is described in a CVPR paper that describes the database, gives detailed information about proper protocols for use, and establishes initial baseline results for the defined protocols [10].

In this paper, we present state-of-the-art results for IJB-A using the bilinear convolutional neural network (BCNN) of Lin et al. [13], after adapting it to our needs, and making a few minor technical changes. We report accuracy on closed-set recognition, and include statistical adaptation to the gallery. We report all statistics required by the IJB-A report including accuracy metrics, enrollment duration, search duration, and template size.

## 1.1 The IARPA Janus benchmark A

There are four key aspects of IJB-A that are relevant to this paper:

1. As stated above, it focuses on identification rather than verification.
2. It includes a wider range of poses than LFW, made possible in part by the fact that images were gathered by hand.
3. The data set includes both video clips and still images.
4. Each “observation” of an individual is dubbed a *template* and may include any combination of still images or video clips. In particular, a single probe is a template and thus typically consists of multiple images of an individual.

These aspects raise interesting questions about how to design a recognition architecture for this problem.

## 1.2 Verification versus identification: adapting to the gallery

Identification is a problem quite different from verification. In *verification*, since the two pictures presented at test time are required to be faces of individuals never seen before, there is no opportunity to build a model for these individuals, unless it is done at test time on the fly (an example of this is the Bayesian adaptation of the probabilistic elastic parts model [12]). Even when such on-the-fly models are built, they can only incorporate a single image or video to build a model of each subject in the test pair.

In identification, on the other hand, at training time the learner is given access to a gallery of subjects with which one can learn models of each individual. While in some cases the gallery may contain only a single image of a subject, in the IJB-A, there are typically many images and video clips of each gallery subject. Thus, there is an opportunity to learn a detailed model (either generative or discriminative) of each subject.

Depending upon the application scenario, it may be interesting to consider identification systems that perform statistical learning on the gallery, and also those that do not. Examples of performing statistical adaptation to the gallery include using the gallery images to adjust the parameters of a model such as a Gaussian mixture model (GMM) or a support vector machine (SVM) to maximize classification accuracy or some other intermediate measure such as likelihood. The chief advantage of *not adapting* to the gallery is faster enrollment times, since the model does not have to be retrained for each new person that is added to the gallery. This can be a critical factor in practice when gallery sizes are very large, when training is very time consuming, or when system requirements necessitate real-time additions to the gallery.

In this work, adaptation to the gallery is a critical aspect of our performance. We report model size and enrollment duration as a function of the current gallery size as part of our evaluation.

### 1.3 Verification as identification

Note that verification can be viewed as an extreme case of identification. In particular, let a pair of test images in verification be called  $(A, B)$ . The image  $A$  can be viewed as a single image of a one person gallery, containing only person  $A$ . Then person  $B$  is either the same as person  $A$ , i.e., matches to person  $A$  of the gallery, or person  $B$  is not in the gallery. Hence, this interpretation of verification falls into the “open set” type of identification.

Despite the fact that verification can be interpreted as a type of identification, the two problems are still justifiably distinct, since having only a single training instance in the above example limits the type of statistical adaptation that can be done. In addition, the fact that the “gallery image” is only obtained at test time (in the verification scenario) may limit the types of model building one might want to do, since there are often more stringent latency restrictions at test time than at training.

### 1.4 Pose variability

Another interesting aspect of IJB-A is the significant pose variability. Because the images were selected by hand, the database does not rely on a fully automatic procedure for mining images, such as the images of LFW, which were selected by taking the true positives of the Viola-Jones detector.

This greater pose variability suggests two important requirements for a successful identification system:

- The representation needs to be flexible enough to deal with a wide range of poses.
- Ideally, the architecture should have an effective way of combining the information from multiple images in a single gallery template, across templates, or within the template of a probe.

**Estimating 3D models.** One way to address pose is to build 3D models [9]. In principle, a set of gallery images can be used to generate a 3D physical model of a head containing all of the appearance information about the gallery identity. Building such 3D models from 2D images or videos is extremely challenging and includes issues such as dealing with lighting, camera parameters, and background as nuisance parameters; dealing with non-rigid distortions of the skin and face caused by expression changes; dealing with the variability of hair and other objects that may occlude parts of the face; addressing variable face parameters such as facial hair, tanning, reflectivity of skin, and flushing; and dealing with the translucency of skin. A generative model that can replicate these varied parameters and is faithful to the appearance of a single individual has an enormous number of parameters. Current methods which take this approach must make a number of simplifying assumptions (such as the rigidity of the head) in order to get reasonable results.

**Frontalization.** Another approach to dealing with large pose variability is to re-render all faces from a canonical point of view, typically from a frontal pose. While this can be done using the above method of estimating a 3D model first, it can also be done directly, without such 3D model

estimation, as done by [21]. This strategy has proven effective for obtaining high performance on benchmarks like LFW. It is still not clear whether such approaches can be extended to deal with the significantly higher variability of databases like IJB-A.

**Averaging descriptors.** Other authors have found that building a generic descriptor for each image, and simply averaging these descriptors across images in a template is surprisingly effective [17]. This has yielded excellent performance in the case of verification on LFW. However, there are clear vulnerabilities to this approach. In particular, if a subject template contains large numbers of image from a particular point of view, as is common in video, such averaging may “overcount” the data from one point of view and fail to incorporate information from another point of view due to its low frequency in a template.

**Multi-view CNN.** Another intriguing possibility is to build a representation which, given a particular feature representation, selects the “best” of each feature across all the images in a template. This is an approach used by the multi-view CNN of Su et al. [19] and applied to the recognition of 3D objects, given multiple views of the object. We adopt some elements of this approach in our method described below.

## 1.5 Face identification as fine-grained classification

In assessing architectures for face identification, it seems natural to consider the subarea of *fine-grained classification*. Fine-grained classification problems are characterized by small or subtle differences among classes, and often large appearance variability within classes. Popular fine-grained benchmarks include such data sets as the CUB data set of bird species identification [23], in which each species is considered a different class. Some pairs of species, such as different types of gulls, have many features in common and can only be discriminated by subtle differences such as the appearance of their beaks.

Face recognition can also be viewed as a fine-grained classification problem, in which each individual represents a different class. It has been observed many times that within class variance is large and between class variance is often subtle in face recognition problems. This makes face recognition a natural member of the fine-grained recognition class of problems.

Recently, Lin et al. [13] have developed the bilinear CNN (B-CNN) model specifically for addressing fine-grained classification problems. It thus seems a natural fit for the face identification problem. By adapting the B-CNN model to the IJB-A data set, we are able to exceed the performance reported for the closed set recognition tasks, as reported in the initial IJB-A report.

In the next section, we give a brief introduction to convolutional neural nets in general. Then in Section 3, we describe the bilinear CNN of Lin et al. [13]. In Section 4, we discuss experiments and results, and we end in Section 5 with some conclusions.

## 2 Introduction to CNNs

Convolutional neural networks (CNNs) are composed of a hierarchy of units containing a convolutional, pooling (e.g. max or sum) and non-linear layer (e.g. ReLU  $\max(0, x)$ ). In recent years deep CNNs typically consisting of the order of 10 or so such units and trained on massive labelled

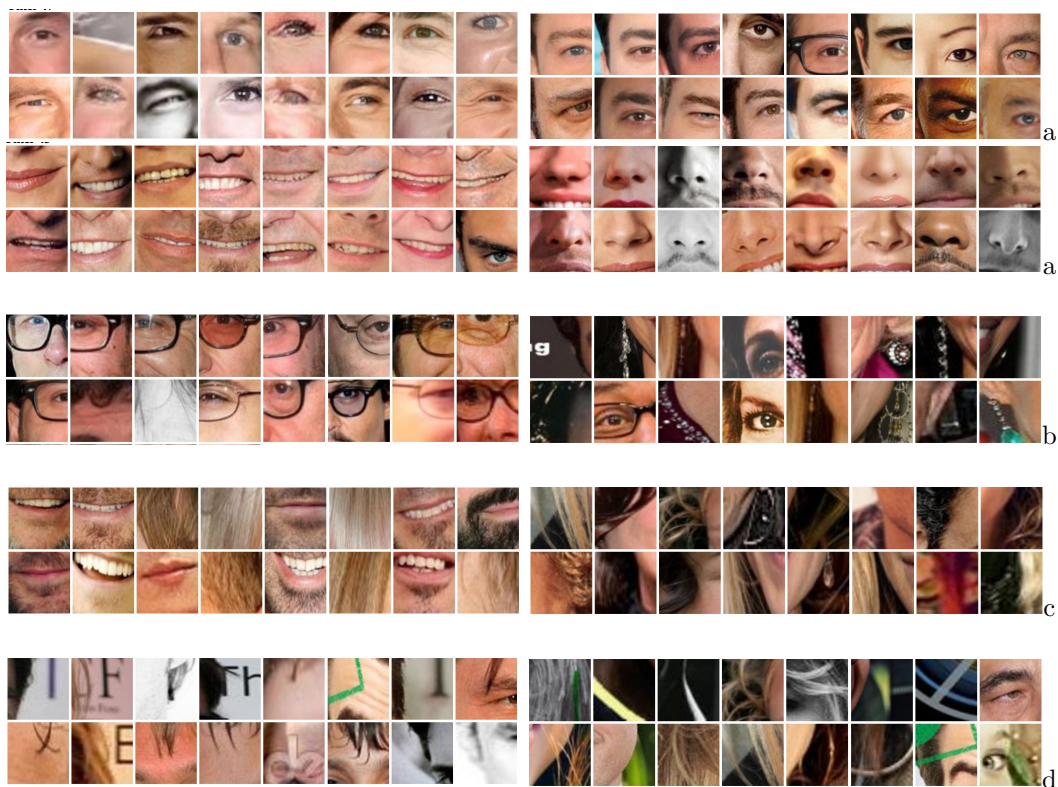


Figure 1: Filters learned from the bilinear CNN. Each 2x8 group of image patches shows the responses of a particular BCNN filter trained on the FaceScrub data set [15]. **a.** The first 4 sets of filter responses show traditional facial features such as eyes, eyes+eyebrows, partially open mouth, and noses. **b.** The BCNN also learns categories of features that seem to be related to accessories, such as eyeglasses and jewelry. **c.** The features in this row seem to be correlated with hair (both facial hair and hair on the top of the head). **d.** Finally, these features are associated with possibly informative aspects of the background such as text and spurious lines.

datasets such as ImageNet have yielded generic features that are applicable in a number of recognition tasks ranging from image classification [11], object detection [5], semantic segmentation [6] to texture recognition [2].

In the domain of fine-grained recognition such as identifying the breed of a dog, species of a bird, or the model of a car, these architectures when combined with detectors that localize various parts of the object have also yielded state-of-the-art results. Without the part-localization, CNNs typically don't perform as well since there is a tremendous variation in appearance caused due to different poses instances of a category can be in that overwhelms the subtle differences across categories. However the drawback of these approaches is that (a) they require manual annotation of parts which can be time consuming (b) require detecting parts which can be computationally expensive.

In contrast models originally developed for texture recognition such as Bag-of-Visual Words (BoVM) [3] and their variants such as the Fisher vector [18] or VLAD [8] have also demonstrated good results on fine-grained recognition tasks. These models don't have an explicit modeling of parts, nor do they require any annotations making them easily applicable to new domains. Deep variants of Fisher vectors [2] based on features extracted from the convolutional layers of a CNN trained on ImageNet [4] provide a better alternative to those based on hand-crafted features such as SIFT [14]. However, pose normalization such as "frontalization" for faces, or part detection for birds, followed by a CNN trained for fine-grained recognition outperforms these texture models. See for example DeepFace of Facebook [21], or pose-normalized CNNs for birds species identification [1, 25].

### 3 Bilinear CNNs

The bilinear CNN models originally introduced by [13] bridge the gap between the texture models and part-based CNN models and consists of two CNNs whose outputs are multiplied (using outer product) at each location of the image. The resulting bilinear feature is pooled across the image resulting in a orderless descriptor for the entire image. This vector can be normalized to provide additional invariances. In our experiments we follow the same protocol as [13] and perform signed square-root normalization ( $\mathbf{y} \leftarrow \text{sign}(\mathbf{x})/\sqrt{|\mathbf{x}|}$ ) and then  $\ell_2$  normalization ( $\mathbf{z} \leftarrow \mathbf{y}/\|\mathbf{y}\|$ ).

The outer product can be viewed as a product of a part and feature detectors both of which are extracted using CNNs, just the sort of thing the pose-normalized architectures try to model. At the same time, this can also be viewed as the local computations of a Fisher vector model, where Gaussian mixture models (GMMs) are used to model clusters of local appearance (often resembling parts) and to a rough approximation the local features are combined with the soft membership to these clusters using an outer product.

The key advantage is that the bilinear CNN model can be trained using only image labels without requiring ground-truth part-annotations. Since the resulting architecture is a directed acyclic graph (DAG), both the networks can be trained simultaneously by back-propagating the gradients of a task-specific loss function. This allows us to initialize generic networks on ImageNet and then fine-tune them on face images. Instead of having to train a CNN for face recognition from scratch, which would require both a search for an optimal architecture and a massive annotated database, we can use pre-trained networks and adapt them to the task of face recognition.



Figure 2: Visualization of *conv5* filters learned from B-CNN model trained only on IJB-A Train set images. Even with limited training data, we can see semantically meaningful and correlated filters are being learned.

## 4 Experiments

### 4.1 Dataset and protocol

The **IJB-A** protocol [10] provides three sets of data for each of its 10 splits. Models can be learned on the Train set, which contains 333 persons with varying number of images, including video frames, per person. The Probe and Gallery sets contain 167 persons disjoint from those in the Train set. We focus on the recognition or search portion of the protocol, where we report *rank-1* and *rank-5* performance of *closed-set search* on the Gallery templates using Probe templates across the 10 splits of the dataset. We perform statistical learning on the Gallery (*Gallery-training*) by training one-versus-all linear SVMs on the identities in the Gallery set.

The **FaceScrub** dataset [15] is an open-access database of face images of actors and actresses on the web, provided as hyperlinks from where the actual images can be downloaded. It contains 530 persons with 107,818 still images in total. There are on average 203 images per person. In an additional experiment, we use this external data to first fine-tune the networks, before subsequent fine-tuning on the IJB Train data. All overlapping identities between the two datasets are removed from FaceScrub before training the networks on it. As some of the download links provided in FaceScrub were broken (and after overlap removal) we finally train the networks on 513 identities, having a total of 89,045 images.

## 4.2 Methods

### Network architectures

As a baseline for deep models, we use the Imagenet-pretrained “M-net” model from VGG’s Mat-ConvNet [22]. All results using this network architecture are hereafter referred to as “**CNN**”. We consider the network outputs of the fully-connected layer after rectification, i.e. layer-19 (‘fc7’ + ‘relu7’) to be used as the face descriptor. An input image is resized to  $224 \times 224$  following the way the network had been initially trained on Imagenet, resulting in a 4096-dimensional feature vector.

We use a symmetric bilinear-CNN model, denoted from now on as “**B-CNN**”, that has both Network A and Network B set to the “M-net” model. Similar to the procedure followed in [13], the bilinear combination is done by taking the rectified outputs of the last convolutional layer in each network, i.e. layer-14 (‘conv5’ + ‘relu5’). We chop off both the networks at layer 14, add the bilinear combination layer, two layers for square-root and L2 normalization and then a softmax layer for classification. For this architecture, the image is upsampled to be  $448 \times 448$ , resulting in a  $27 \times 27 \times 512$  output from each network at layer-14 (  $27 \times 27$  are the spatial dimensions of the response map and 512 denotes the number of CNN filters at that layer). The bilinear combination results in a  $512 \times 512$  output, and its vectorization (followed by the normalization layers mentioned earlier) gives us the final face descriptor.

### Network fine-tuning

Even though the models were trained initially for large-scale image classification on the Imagenet dataset, fine-tuning the networks for the specific task of face recognition is expected to significantly boost performance. We consider four different scenarios with respect to fine-tuning:

- *no-ft*: No fine-tuning is done. We simply use the Imagenet-pretrained model without any retraining on the IJB-A data as a baseline for our experiments.
- *Train*: The networks are fine-tuned on the Train set of the IJB-A data. We fine-tune the CNN models by replacing the last layer with a softmax, setting its learning rate to be 10 times the learning rate for the lower layers and running back-propagation with dropout regularization for 25 epochs. The stopping time is determined when the validation error remains constant even after learning rate is changed. The B-CNN is similarly fine-tuned for 50 epochs on the Train set. It is to be noted that the identities which the networks are being trained to classify here are disjoint from the identities present in the test set.
- *FaceScrub*: The B-CNN is fine-tuned on FaceScrub data for 70 epochs and the CNN for 25,
- *FaceScrub+Train*: The FaceScrub data provides a good initialization for the face identification task to the networks, following which we fine-tune on the Train set for 50 epochs.

### Classifiers and pooling

One-versus-All linear SVM classifiers are trained on the Gallery set for all our experiments. We do not do any form of template-pooling at this stage and simply consider each image or video frame of a person as an individual sample. The weight vectors of the classifiers are rescaled such that the median scores of positive and negative samples are -1 and +1. Since all evaluations on this protocol are to be reported at the template level, we have the following straightforward strategies for pooling the media (images and video-frames) within a template at test time:



- *Score pooling*: We use the MAX operation to pool the SVM scores of all the media within a Probe template. This is done after SVM scores are computed for each individual image or frame that comprises a template.
- *Feature pooling*: The MAX operator is applied on the features this time to get a single feature vector for a template. Thus, the SVM is run only once per Probe template.

## 5 Results

As specified in the IJB-A description document [10], we report the relevant parameters for the **search** paradigm of the database under the **closed set** protocol. *Cumulative-Match-Characteristic* (CMC) curves for our final B-CNN model are also included (see Figure 3).

### Comparison of fine-tuning methods

We first compare our approach to the baseline CNN model. Table 1 reports the rank-1 and rank-5 accuracy with different fine-tuning approaches. Without fine-tuning, CNN achieves 24.1% and B-CNN achieves 26.3% accuracy with score pooling, and CNN achieves 24.2% and B-CNN achieves 25.7% using feature pooling respectively. When fine-tuning on IJB-A train set, networks learn the convolutional filters specific for faces. Performance improves more than 17% both for CNN and B-CNN. In this case, B-CNN achieves better results than CNN by a margin for both score pooling (45.8% vs. 41%) and feature pooling (44.6% vs. 41.1%).

In a second network-training pipeline, we first learn a good representation for the task of face identification using the FaceScrub dataset. After this, fine-tuning on the IJB-A Train set is performed as before. Accuracy is much higher when the initial training of networks is done on an external face dataset with adequate training data.

Rank-1	CNN		B-CNN	
	score pooling	feature pooling	score pooling	feature pooling
no-ft	0.241 $\pm$ 0.030	0.242 $\pm$ 0.025	0.263 $\pm$ 0.026	0.257 $\pm$ 0.030
Train	0.410 $\pm$ 0.020	0.411 $\pm$ 0.017	0.446 $\pm$ 0.020	0.458 $\pm$ 0.022
FaceScrub	0.380 $\pm$ 0.020	0.403 $\pm$ 0.019	0.483 $\pm$ 0.014	0.492 $\pm$ 0.017
FaceScrub+Train	0.490 $\pm$ 0.021	0.484 $\pm$ 0.022	0.538 $\pm$ 0.017	0.551 $\pm$ 0.022
Rank-5	CNN		B-CNN	
	score pooling	feature pooling	score pooling	feature pooling
no-ft	0.449 $\pm$ 0.027	0.425 $\pm$ 0.021	0.434 $\pm$ 0.026	0.427 $\pm$ 0.022
Train	0.648 $\pm$ 0.023	0.639 $\pm$ 0.174	0.669 $\pm$ 0.015	0.676 $\pm$ 0.018
FaceScrub	0.604 $\pm$ 0.023	0.629 $\pm$ 0.023	0.696 $\pm$ 0.014	0.691 $\pm$ 0.014
FaceScrub+Train	0.726 $\pm$ 0.023	0.712 $\pm$ 0.021	0.757 $\pm$ 0.021	0.757 $\pm$ 0.016

Table 1: Showing **rank-1** and **rank-5** retrieval rates of CNN and B-CNN with different pooling schemes and various levels of fine-tuning. Fine-tuning the networks on the larger FaceScrub dataset followed by fine-tuning on the provided IJB-A train set provides a considerable boost to performance. Simply pooling features using the MAX operation either outperforms or gets comparable accuracy to max-pooling SVM scores.

### Comparison of template-pooling methods

We also evaluate two pooling schemes in Table 1 at score and feature level using rank-1 and rank-5 retrieval rates. For the CNN network, the two pooling schemes achieve almost the same accuracy, while feature pooling either outperforms score pooling or has negligible difference when using fine-tuned B-CNN models. The reason for the preference of feature pooling on B-CNN is that the model learns good semantic part filters by fine-tuning (see Figure 1, Figure 2) and feature pooling combines the part detections which might be invisible from a particular viewpoint by taking the maximum part detection response across views when a sequence of faces (with different views) is provided.

At higher ranks however, we see that the score pooling is slightly better than feature pooling (83.65% versus 83.30% at rank-10, see Figure 3). Even so, for efficiency considerations, it is better to pool a large number of features into a single compact template and then perform classification on this template representation, than individually evaluating scores for each image or video frame in a template and then pooling the scores.

### Comparison to GOTS and OpenBR

In Table 2, we compare B-CNN with the methods reported in [10]. Since the other methods are not fine-tuned on the IJB-A data, we categorize them in the *no-ft* section of the table. Using freely available ImageNet pre-trained models and a modest external database of faces, we substantially outperform the reported methods. The bilinear CNN model also consistently outperforms the regular CNN model.

	GOTS		OpenBR		B-CNN	
	rank 1	rank 5	rank 1	rank 5	rank 1	rank 5
no-ft	$0.443 \pm 0.021$	$0.595 \pm 0.020$	$0.246 \pm 0.011$	$0.375 \pm 0.008$	$0.257 \pm 0.030$	$0.427 \pm 0.022$
Train	-	-	-	-	$0.458 \pm 0.022$	$0.676 \pm 0.018$
FaceScrub	-	-	-	-	$0.492 \pm 0.017$	$0.691 \pm 0.014$
FaceScrub+Train	-	-	-	-	$0.551 \pm 0.022$	$0.757 \pm 0.016$

Table 2: We compare the performance of B-CNN model and the other methods reported in [10]. Here we use *feature pooling* in the B-CNN.

### Run-time and feature size information

The B-CNN encoding time for a single image is roughly 0.0764 seconds. The SVM training on entire Gallery takes around 50 minutes on average using the 262,144-dimensional features. The pooling methods depend largely on the number of images comprising a single template. On average the feature pooling is 2 times faster than score pooling at negligible difference in accuracy.

## 6 Discussion

It is perhaps not surprising that CNN architectures that have succeeded on other fine-grained recognition problems also do well at face identification. There are a number of directions to continue exploring these models. These include:

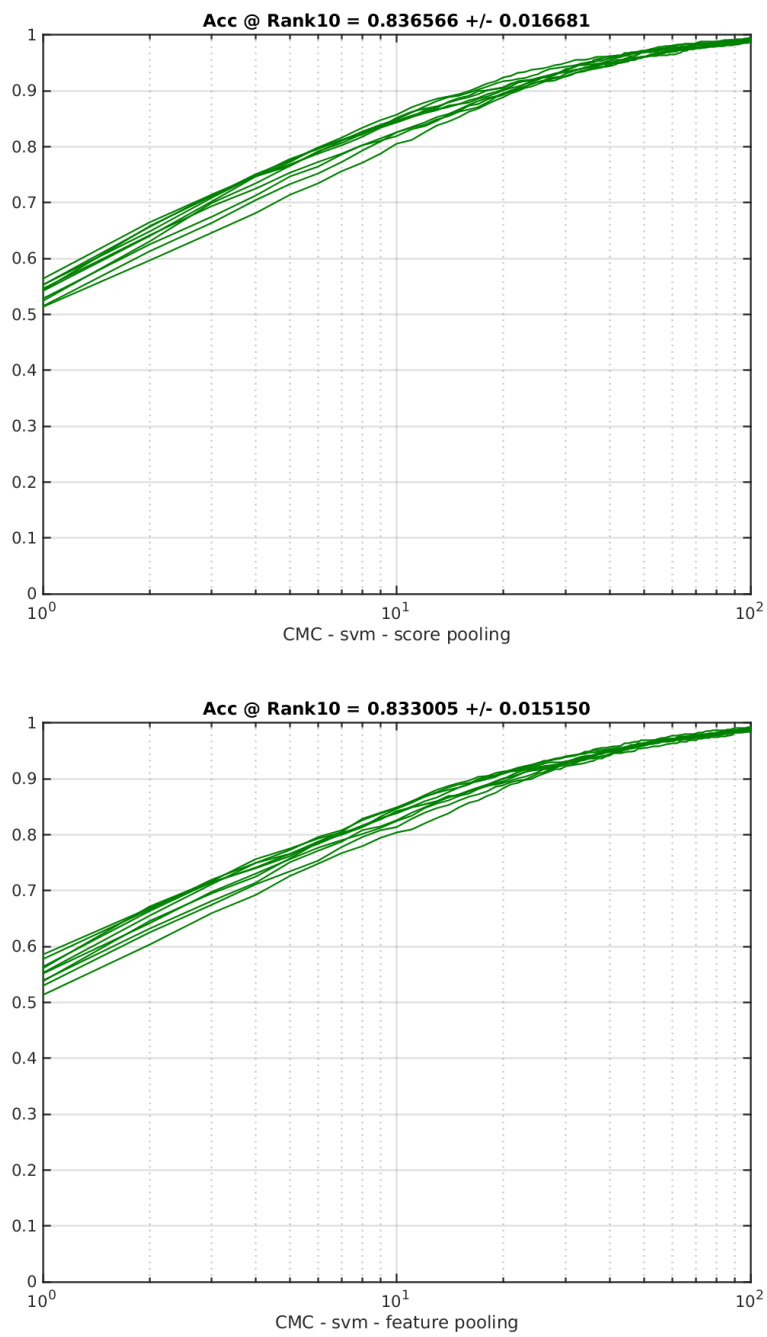


Figure 3: CMC curves for all 10 splits using the B-CNN model fine-tuned on both FaceScrub and IJB-A train set.

- retraining the entire model using an objective similar to the multi-view CNN objective in which the weights for the network are learned under the assumption that the max will be taken across images in a template,
- Exploring additional architectural parameters, such as stride, layer size, and number of layers, to further improve results,
- using “pre-training” sets much larger than FaceScrub, such as the CASIA WebFaces with 10,000 identities, to further improve the fine-tuning performance,
- using a bottle-neck layer after bilinear pooling layer to reduce the feature dimension.

We believe the success of the BCNN relative to non-bilinear architectures makes them a sensible starting point for a wide variety of continued experiments.

## 7 Acknowledgements

This research was supported in part by the Office of the Director of National Intelligence (ODNI), Intelligence Advanced Research Projects Activity (IARPA) under contract number 2014-14071600010.

## References

- [1] S. Branson, G. V. Horn, S. Belongie, and P. Perona. Bird species categorization using pose normalized deep convolutional nets. In *Proc. BMVC*, 2014.
- [2] M. Cimpoi, S. Maji, and A. Vedaldi. Deep filter banks for texture recognition and description. In *Proc. CVPR*, 2015.
- [3] G. Csurka, C. R. Dance, L. Dan, J. Willamowski, and C. Bray. Visual categorization with bags of keypoints. In *Proc. ECCV Workshop on Stat. Learn. in Comp. Vision*, 2004.
- [4] J. Deng, W. Dong, R. Socher, L.-J. Li, K. Li, and L. Fei-Fei. ImageNet: A large-scale hierarchical image database. In *Proc. CVPR*, 2009.
- [5] R. B. Girshick, J. Donahue, T. Darrell, and J. Malik. Rich feature hierarchies for accurate object detection and semantic segmentation. In *Proc. CVPR*, 2014.
- [6] B. Hariharan, P. Arbeláez, R. Girshick, and J. Malik. Simultaneous detection and segmentation. In *Proc. ECCV*. 2014.
- [7] G. B. Huang, M. Ramesh, T. Berg, and E. Learned-Miller. Labeled faces in the wild: A database for studying face recognition in unconstrained environments. Technical report, 07-49, University of Massachusetts, Amherst, 2007.
- [8] H. Jégou, M. Douze, C. Schmid, and P. Pérez. Aggregating local descriptors into a compact image representation. In *Proc. CVPR*, 2010.
- [9] I. Kemelmacher-Shlizerman and R. Basri. 3D face reconstruction from a single image using a single reference face shape. *PAMI*, 2011.

- [10] B. F. Klare, B. Klein, E. Taborsky, A. Blanton, J. Cheney, K. Allen, P. Grother, A. Mah, M. Burge, and A. K. Jain. Pushing the frontiers of unconstrained face detection and recognition: IARPA Janus Benchmark A. In *Proc. CVPR*, 2015.
- [11] A. Krizhevsky, I. Sutskever, and G. E. Hinton. Imagenet classification with deep convolutional neural networks. In *Proc. NIPS*, 2012.
- [12] H. Li, G. Hua, Z. Lin, J. Brandt, and J. Yang. Probabilistic elastic matching for pose variant face verification. In *Proc. CVPR*, 2013.
- [13] T.-Y. Lin, A. Roy Chowdhury, and S. Maji. Bilinear CNN models for fine-grained visual recognition. *arXiv preprint arXiv:1504.07889*, 2015.
- [14] D. G. Lowe. Object recognition from local scale-invariant features. In *Proc. ICCV*, 1999.
- [15] H.-W. Ng and S. Winkler. A data-driven approach to cleaning large face datasets. In *Proc. ICIP*, 2014.
- [16] E. Nowak and F. Jurie. Learning visual similarity measures for comparing never seen objects. In *Proc. CVPR*, 2007.
- [17] O. M. Parkhi, K. Simonyan, A. Vedaldi, and A. Zisserman. A compact and discriminative face track descriptor. In *Proc. CVPR*, 2014.
- [18] F. Perronnin, J. Sánchez, and T. Mensink. Improving the Fisher kernel for large-scale image classification. In *Proc. ECCV*, 2010.
- [19] H. Su, S. Maji, E. Kalogerakis, and E. Learned-Miller. Multi-view convolutional neural networks for 3D shape recognition. *arXiv e-prints*, abs/1505.00880, May 2015.
- [20] Y. Sun, Y. Chen, X. Wang, and X. Tang. Deep learning face representation by joint identification-verification. In *Proc. NIPS*, 2014.
- [21] Y. Taigman, M. Yang, M. Ranzato, and L. Wolf. Deepface: Closing the gap to human-level performance in face verification. In *Proc. CVPR*, 2014.
- [22] A. Vedaldi and K. Lenc. Matconvnet-convolutional neural networks for matlab. *arXiv preprint arXiv:1412.4564*, 2014.
- [23] P. Welinder, S. Branson, T. Mita, C. Wah, F. Schroff, S. Belongie, and P. Perona. Caltech-UCSD Birds 200. Technical Report CNS-TR-2010-001, California Institute of Technology, 2010.
- [24] L. Wolf, T. Hassner, and I. Maoz. Face recognition in unconstrained videos with matched background similarity. In *Proc. CVPR*, 2011.
- [25] N. Zhang, R. Farrell, and T. Darrell. Pose pooling kernels for sub-category recognition. In *Proc. CVPR*, 2012.